ACS APPLIED MATERIALS & INTERFACES

Research Article

www.acsami.org

Colloidal Transfer Printing

Michael J. Skaug,[†] Brennan M. Coffey,[†] and Daniel K. Schwartz*

Department of Chemical and Biological Engineering, University of Colorado Boulder, Boulder, Colorado 80309, United States

Supporting Information

ABSTRACT: Many fields of research have adopted self-assembly of colloidal spheres as an easy and reliable method to produce macroscopic structures with nanoscale periodicity. The field of soft lithography in particular has used colloidal self-assembly to fabricate lithographic masks and templates. We developed a colloidal lithography method that uses the colloidal assembly directly to produce submicrometer topographic and chemical surface patterns. The method does not require any specialized equipment, making it particularly useful in biological and chemical laboratories without lithography expertise. The technique involves the curing and solvent removal of a self-assembled colloidal crystal from an inorganic surface. The result is a triangular array of polymer features with submicrometer periodicity that covers square centimeters of surface area. The feature size and spacing is easily controlled, and the features serve as reactive sites for biomolecule immobilization.

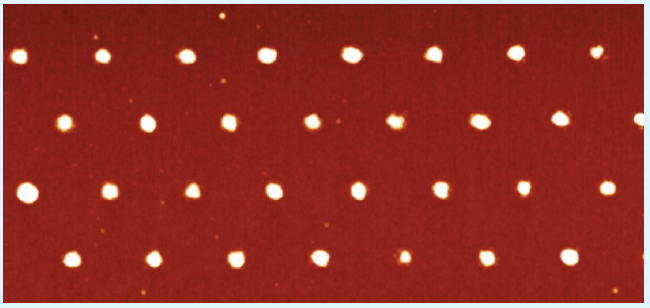

KEYWORDS: *soft lithography, colloidal lithography, surface patterning, protein array*

INTRODUCTION

Nanoscale surface patterning is required in many technological fields, including biotechnology where protein, DNA, and cell arrays are used to study chemical recognition and cell−surface interactions, and screen pharmaceuticals.[1−3] For example, controlling the spatial distribution of cell-binding ligands on a substrate provides insight into cell proliferation, differentiation, and mobility, which guides the development of new biomaterials.[4,5] An array of cells on a surface can also act as a sensitive detector of environmental pathogens[6,7] or as a device for screening new pharmaceuticals.[8]

To produce chemical and topographic surface patterns, there are many available techniques. Traditional lithography uses high-energy particles, such as photons,[9] electrons,[10] and ions,[11] to pattern a surface. Photolithography is ubiquitous in electronics manufacturing, because it enables high-throughput patterning of complex feature geometries. Electron-beam and ion-beam lithographies have excellent resolution and can produce arbitrary patterns, but they are slow and impractical for patterning macroscopic areas. Despite their strengths, traditional lithographic techniques suffer from limitations that prevent them from being used frequently in bench-scale experiments, particularly in the biological and chemical fields. The primary limitation is cost. Traditional lithography requires substantial capital investment, and even when the resources are available, designing and testing new patterns can be slow.

As an alternative to standard photolithography, a class of techniques known as soft lithography has been developed.[9,12,13] It has been widely adopted in biotechnological fields because it allows for rapid prototyping and relies primarily on wet chemical processes. Most soft lithographic methods use a master, fabricated with traditional lithography, to mold a polymer stamp, which is then used to add or remove material from a surface. Except for the initial fabrication of the master, soft lithography is fast and low cost. Colloidal lithography is a branch of soft lithography that avoids the need for a master altogether by taking advantage of the ease and reproducibility of colloidal self-assembly[14] to produce submicrometer surface patterns and structures.[15] In colloidal lithography, a close-packed array of polymer spheres functions as a mask or template for the deposition or removal of material.[15−21] For example, a close-packed array of particles can be used to mask the evaporative deposition of a metal, so that after removing the colloidal particles, an ordered array of metal nanostructures is left on the surface.[21] Colloidal lithography has also been adopted as a method to mask the deposition of a self-assembled monolayer in order to create patterned surface chemistry.[16]

Rather than use the colloidal crystal as a mask or template for later removal, we present a new lithographic method, colloidal transfer printing, which directly transfers material from colloidal particles to the substrate. This simple procedure involves depositing a close-packed array of polymer spheres, curing at elevated temperature, and removal in solvent. Thus, it complements standard colloidal lithography, requires few processing steps, and only requires equipment common to most chemical and biological laboratories. The result is an array of polymer features approximately 100 nm in size and with submicrometer spacing. The feature size and spacing can be easily controlled through the curing temperature and colloidal particle size, respectively. The chemistry of the surface features

Received: July 9, 2013
Accepted: November 25, 2013
Published: November 25, 2013

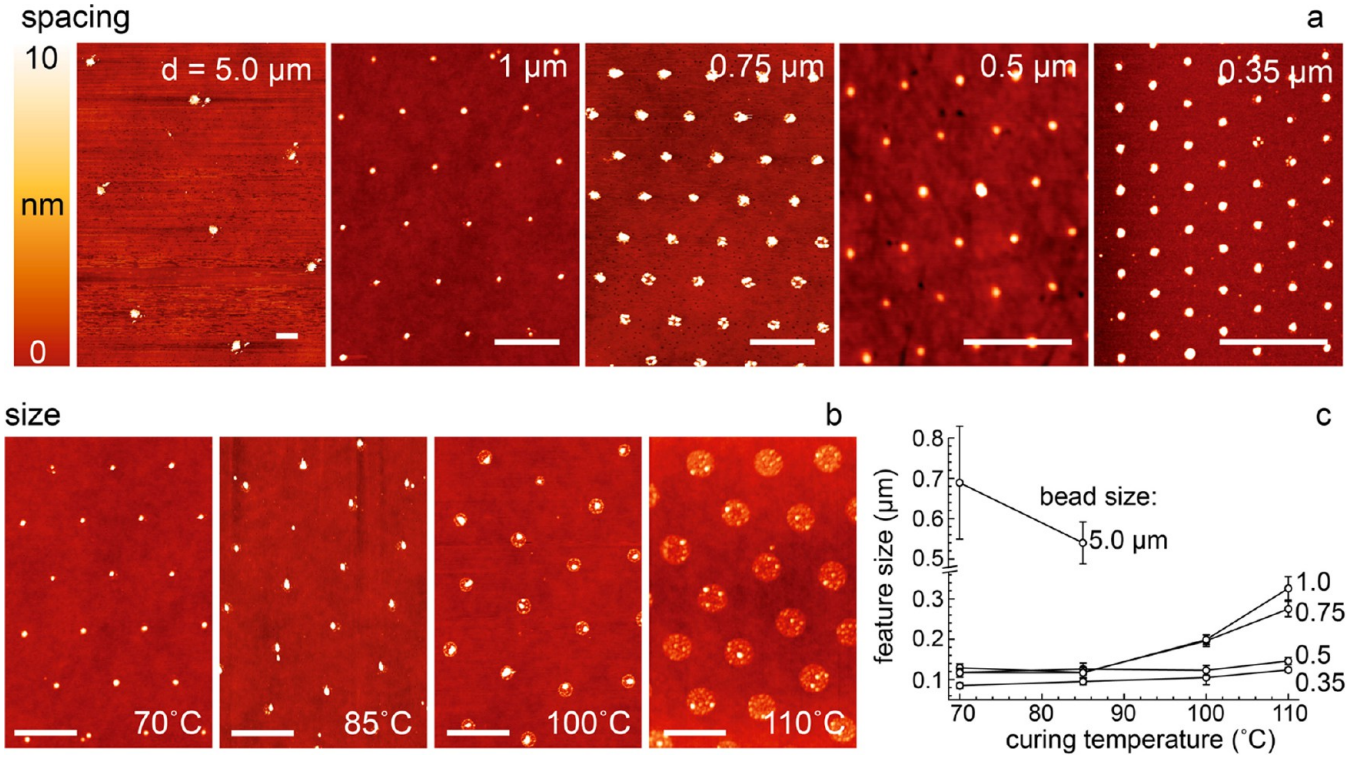

Figure 1. (a) AFM images of colloidal transfer patterns with different feature spacings, *d*, as annotated. (b) The effect of curing temperature on feature size. AFM images of 1 μm patterns heated at the annotated temperature before sonication. All scale bars are 1 μm. (c) The influence of bead size and curing temperature on the feature size.

depends on the composition of the original polymer particles, so it can be tuned by using different polymer chemistries to produce a functional surface pattern.

MATERIALS AND METHODS

Colloidal Transfer Printing. A close-packed array of polystyrene spheres was created by drying a droplet of colloidal suspension on a cleaned substrate using established methods.[16] The substrates were either borosilicate glass coverslips (Fisher Scientific) or polished silicon wafers (Electrooptic Materials) that were cleaned by immersion in Piranha (1:3 v/v 30% aqueous H_2O_2 (Fisher Scientific) to H_2SO_4 (Fisher Scientific)) solution at 80 °C for 1 h, followed by exposure to UV−ozone (Boekel Ind.) for 1 h. *(CAUTION: "Piranha" solution reacts violently with organic materials; it must be handled with extreme care.)* After cleaning, approximately 100 μL of a colloidal suspension was pipetted onto the surface. A variety of colloidal particles was tested. The most frequently used was the carboxylate modified latex particle (CML, 4% w/v CML Latex, Life Technologies) that was a copolymer of acrylic acid and styrene, which was used as purchased in diameter sizes of 0.35, 0.50, 0.75, 1.00, and 5.00 μm. Carboxyl surface-modified latex (Carboxyl, 4% w/v Carboxyl Latex, Life Technologies) was also tested with particle diameters of 0.50, 0.75, and 1.00 μm. In control experiments, we used a 1.00 μm cross-linked polymer particle (DVB, 4% w/v DVB/Carboxyl Latex, Life Technologies) with carboxyl surface modification and 1.00 μm sulfonate surface-modified polystyrene latex (Sulfonate, 4% w/v Sulfonate Latex, Life Technologies). Further information on particle chemistry and composition was unavailable from the manufacturer. After depositing a droplet of colloidal suspension on the cleaned substrate, the sample was tilted at a shallow angle (~3°) and the colloidal suspension was allowed to dry at ambient conditions, leaving a multilayer, close-packed array of colloidal spheres on the surface. The samples were then cured at elevated temperature (70−110 °C) for 18 h in a chemical oven (Thermo Scientific, IsoTemp).

After curing, the colloidal crystals were allowed to cool to room temperature and were sonicated (FS30, Fisher Scientific) in acetone (Fisher Scientific) or isopropanol (Fisher Scientific) until the surface was visibly clean (~15 min). After sonication, the substrate was continuously rinsed with acetone during removal from the sonication solution and then rinsed with isopropanol (Fisher Scientific) and ultrapure water (>18 MΩ·cm^{-1}). The substrates were then dried with a stream of nitrogen and stored in ambient conditions.

Atomic Force Microscopy. Surface patterns were imaged using a Nanoscope IIIa multimode atomic force microscope (Digital Instruments). Height images were obtained in tapping mode, using silicon cantilevers (RTESPA, Bruker) at ambient conditions. The AFM images were analyzed using Gwyddion (v2.30) and ImageJ (NIH Freeware).

Protein Immobilization. Bovine serum albumin fluorescently labeled with Alexa555 (BSA-555, Life Technologies) was covalently attached to the surface patterns using standard carboxylate-amine cross-linking chemistry.[22] Cross-linking was performed using sulfo-*N*-hydroxysuccinimide (Sulfo-NHS) (Thermo Scientific) and 1-ethyl-3-[3-dimethylaminopropyl]carbodiimide (EDC) (Thermo Scientific). 20 mg of Sulf-NHS and 20 mg of EDC were added to 1 mL of 100 mM MES buffer (2-[morpholino]ethanesulfonic acid, Thermo Scientific) at pH 6.0. The reaction mixture was pipetted onto the patterned substrate and allowed to react for 15 min. The substrate was then rinsed with MES buffer and immersed in MES buffer containing 0.001 mg/mL BSA-555. The contents of the reaction vessel were allowed to react for 4 h with continuous stirring. When the reaction had finished, the substrates were rinsed with MES and transferred to a prewarmed water bath at 65 °C for 15 min to remove nonspecifically adsorbed protein. After 15 min, the volume of the water bath was exchanged with clean water (>18 MΩ·cm^{-1}). Care was taken at this step to avoid bubble formation near the surface of the substrates. The functionalized surfaces were then dried under a stream of nitrogen and stored protected from light.

Fluorescence Microscopy. Patterns functionalized with fluorescent BSA were imaged using epi-fluorescence on a Nikon Eclipse Ti microscope, with a Nikon Plan Apo 100× oil-immersion objective, a 1.0× or 1.5× magnification lens, Photometrics Cascade II512 camera,

and Nikon NIS-Elements AR 4.11.00 software. Images were analyzed using ImageJ (NIH freeware).

RESULTS AND DISCUSSION

After curing and removal of the colloidal particles by sonication in acetone (CML and Carboxyl), we found a residual, triangular array of features on the surface (Figure 1a). The periodic spacing of the features, *d*, was equal to the diameter of the particles used to assemble the colloidal array. The triangular pattern uniformly covered the entire area of the surface originally covered by the colloidal crystal, ~1 cm^2. We believe that the features were polymer deposits from the colloidal particles, left where each particle was in contact with the surface. We propose a mechanism where sonication cleaves the particles that are in contact with the surface, leaving behind a patch of polymer residue (Figure 2).

The proposed mechanism (Figure 2) is based on a balance between particle−surface adhesive forces and intraparticle cohesive forces. At one extreme, where cohesive forces dominate, the particles would remain intact during sonication, and no residue would remain on the surface. This is what we found in a control experiment where, instead of the normal (CML or Carboxyl) polystyrene particles, where intraparticle cohesion is the result of noncovalent interactions, we used cross-linked polystyrene particles (DVB). In this case, no array of surface features was evident (Figure S1, Supporting Information). A similar result was found when we performed the sonication in water, a poor solvent for polystyrene; both Carboxyl and CML colloidal particles were completely removed and no pattern was left on the surface (not shown). At the other extreme, we performed an experiment where we sonicated in toluene, a good solvent for polystyrene,[23] and the Carboxyl and CML particles dissolved, leaving disordered residue on the surface (Figure S2 Supporting Information). However, in a moderate solvent like acetone, the particles are expected to swell but not dissolve. As a result, intraparticle cohesion is reduced, particle−surface adhesion is maintained, and the particles cleave near the point of surface contact. We also found that sonication in isopropanol produced the same results as sonication in acetone. A similar mechanism, i.e., strong surface adhesion promoting the transfer of material, underlies other transfer printing methods.[13,24] The primary advance here is that no master is required and colloidal assembly enables patterning at scales below what could be easily achieved with any other technique.

We can rationalize the above results in terms of the solvent quality of the sonicating liquid. Solvent quality can be estimated on the basis of the Hansen solubility model where each polymer and solvent has three associated solubility parameters.[23] In the three-dimensional solubility parameter space, solvents that are less than 12.7 from polystyrene are defined as good solvents and those farther away are considered to be poor solvents.[25] The distances for the liquids we tested are: 8.57 for toluene, 13.05 for acetone, 20.34 for isopropanol, and 55.88 for water. Toluene is predicted to be a good solvent for polystyrene based on this value, while solvents with values just outside 12.7, such as acetone and isopropanol, have some solvency capability, and liquids with values much larger than 12.7, like water, are poor solvents for polystyrene. This indicates that other moderate solvents for polystyrene would yield similar results, and we hypothesize that solvents like diethyl ether (13.95), DMF (14.89), or isobutanol (20.67) would work similarly to the acetone and isopropanol tested here.[25]

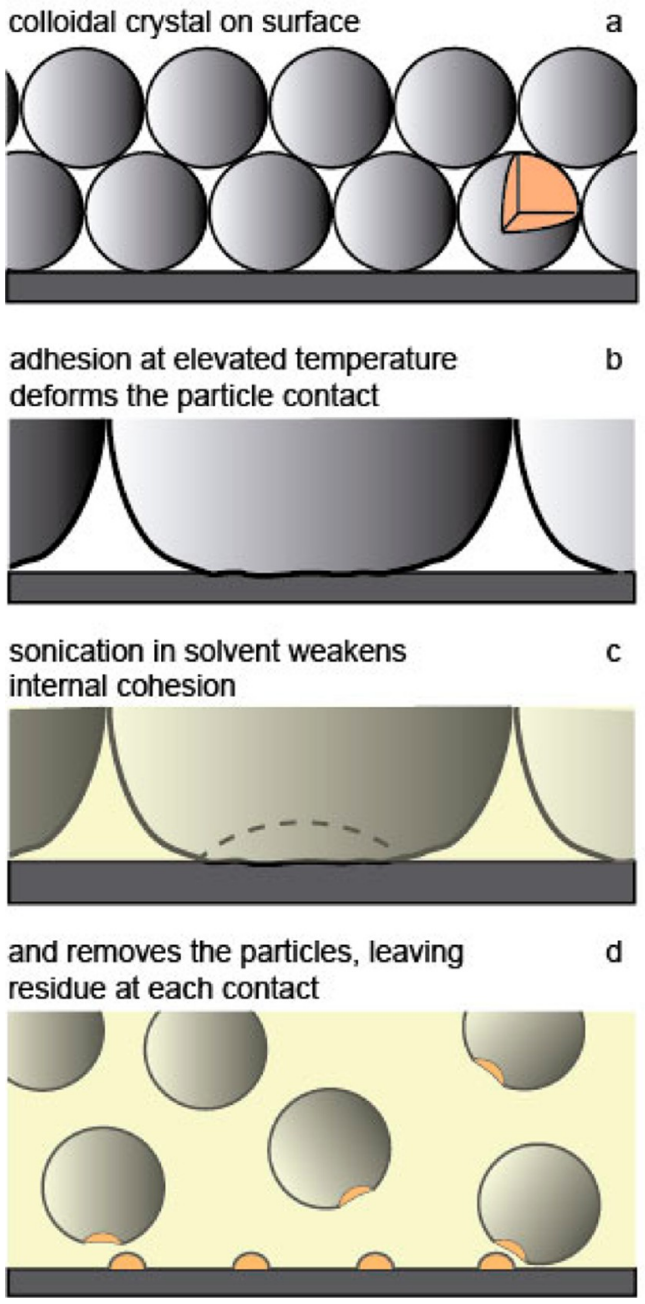

Figure 2. Illustration of the proposed mechanism of pattern deposition. (a) The colloidal crystal formed on the surface. (b) Curing the colloidal crystal at elevated temperature deforms each particle at its adhesive contact with the surface. (c) Sonication in solvent weakens internal particle cohesion. (d) Particles are removed from the surface, leaving a polymer feature at each contact point.

Though we primarily tested carboxyl-modified polystyrene particles (CML and Carboxyl), Sulfonate particles produced similar results (Figure S3, Supporting Information). We also found the same results for slightly different substrates, including fused silica and silicon. These results indicate that the particle−surface adhesion that promotes pattern deposition is likely the result of nonspecific interactions between the polymer and surface. This is also consistent with the requirement that the colloidal crystal be cured at ~70 °C for longer than 12 h before removal. Without curing the colloidal crystal on the substrate, no pattern was transferred (Figure S4, Supporting Informa-

tion). Presumably, curing promotes polymer relaxation near the surface and removal of residual water to promote intimate contact between the particle and surface and increase particle−surface adhesion. On the basis of these results, we expect that many other combinations of particle and surface chemistry could be used with the technique we have developed. The only requirements are that a close-packed array of particles can be assembled on the surface and a suitable solvent is selected.

Feature spacing, *d*, is easily controlled by using colloidal particles of different size. We tested different particle sizes, for both CML and Carboxyl particles, from 0.35 to 5 μm (Figure 1a). We expect that the minimum feature spacing is only limited by the availability of monodisperse colloids of appropriate diameter, although we did not test particles smaller than 0.35 μm. For particles larger than 1 μm, patterning was less uniform. The largest feature spacing investigated was a 5 μm pattern, and while we were able to deposit the triangular array of features (Figure 1a), the array had much smaller regions of order than those patterns prepared with beads whose diameter was less than 1 μm. We also found that, after curing at elevated temperatures, the 5 μm colloidal particles could not be removed during the sonication step, consistent with the much larger particle−surface contact area discussed below. The wide range of feature spacings highlights one of the primary strengths of this technique: patterns with submicrometer feature size and spacing can be created without the need for any specialized equipment beyond what would be found in a normal wet laboratory.

There was some variability in height of the features and occasional defects in the transferred pattern (Figure 1a). On the basis of the proposed mechanism of pattern transfer (Figure 2), we expect that the feature size and uniformity intimately depend on the colloidal particle composition, which would determine particle adhesion and cohesion. For example, slight changes in polymer molecular weight or chemistry (which might be expected between batches of commercial colloidal particles) would change the cohesive properties of the colloidal particles. Substrate heterogeneity could also influence the uniformity of particle−surface adhesion, so although we used standard, commercially available substrates and colloidal particles, pattern uniformity might be improved through greater control over surface and particle properties.

In addition to controlling the feature spacing using different particle sizes, the feature size can also be controlled by curing the colloidal crystal at different temperatures. The glass transition temperature of polystyrene is $T_g \approx 100$ °C,[23] and curing the particles at or above the glass transition resulted in a larger feature size being left after sonication (Figure 1b,c). The feature size reflects the contact area between the particle and the surface. The contact area is determined by the contact mechanics of the particle−surface interaction, which is described by the so-called JKR theory.[26] Particle deformation is promoted by particle−surface adhesion but resisted by the particle elasticity, and the resulting contact radius, *R*, is predicted to scale with the particle elastic modulus, *E*, like $R \sim E^{-1/3}$.[26] Thus, at equilibrium, the area of contact between a sphere and a flat surface increases with decreasing particle elastic modulus. For the polystyrene particles studied here, the elastic modulus is a decreasing function of temperature. Below the glass transition temperature, the elastic modulus decreases slowly with increasing temperature. For example, the modulus decreases by approximately 2% over the temperature range of 70 to 85 °C,[23] and thus, the contact radius is only expected to increase by a factor of about 0.007. However, near the glass transition temperature, the particle modulus decreases more quickly, changing by about 50% over the range of 85 to 110 °C,[27] with a consequent 25% increase in contact radius. Although we observed larger increases in feature sizes in some cases, we only observed measurable increases when curing at 100 or 110 °C (Figure 1c), which is consistent with a mechanism based on an elastic modulus controlled contact area. The deformation of polymer colloids at elevated temperatures has also been previously investigated and used to modify the morphology of colloidal structures.[28−30] For example, when used as a mask for the deposition of a self-assembled monolayer, heating a colloidal crystal above the glass transition temperature resulted in a linear increase in the size of the holes left in the patterned monolayer.[28]

We also investigated the influence of particle diameter on feature size. At low curing temperatures, there was little change in feature size with particle diameter, except for the 5 μm particles, which produced significantly larger feature sizes (Figure 1c). At elevated curing temperatures, there was a noticeable increase in feature size with increasing particle diameter. The larger feature sizes with the 5 μm particles may explain why, after curing at the higher temperatures, they could not be removed during sonication; the much larger area of contact with the surface prevented removal.

Colloidal transfer printing produces a submicrometer array of polymer bumps over large surface areas. The height and regular spacing of the features could potentially be used in work that explores the influence of curvature on cell and lipid membrane behavior.[31,32] This technique also provides a simple route to a large-scale array of polymer features, which could be utilized for their unique chemical properties and functionality.[33] For example, the unique chemistry of the resulting polymer surface pattern could be functionalized with a biomolecule.

As a proof of principle and to demonstrate the utility of the polymer surface pattern, we used the surface features as reactive sites for the surface immobilization of fluorescently labeled BSA. Assuming the mechanism depicted in Figure 2, each polymer feature presented the same chemistry as the bulk polymer of the original colloidal particles although we could not rule out that the original particle surface functionality was also present in the polymer pattern (we point this out because many commercially available colloidal particles have different surface and bulk chemistries). To prepare a reactive surface pattern, we used CML particles with a diameter of 5.0, 1.0, or 0.5 μm. The particles were a copolymer of acrylic acid and styrene, so we expect that some carboxylate groups were exposed in the surface pattern. We then covalently attached BSA to the surface features using a standard amine−carboxylic acid cross-linking reaction (see Materials and Methods).

Fluorescence images of the BSA functionalized 5.0 μm pattern revealed the triangular surface pattern (Figure 3). Images of functionalized 0.5 and 1.0 μm patterns are shown in Figure S6 and S7, Supporting Information, respectively. As mentioned previously, longer-range order was achieved when using the smaller 0.5 and 1.0 μm particles, but the pattern was more evident to the eye in the images of the 5.0 μm pattern. The fluorescence intensity from each spot had an approximately Gaussian profile (Figure S5, Supporting Information) consistent with fluorescence emanating from a feature with a diameter near the diffraction limit (Figure 1c). The Fourier transform illustrates the long-range order across the entire field of view. Some nonspecific adsorption to the substrate between

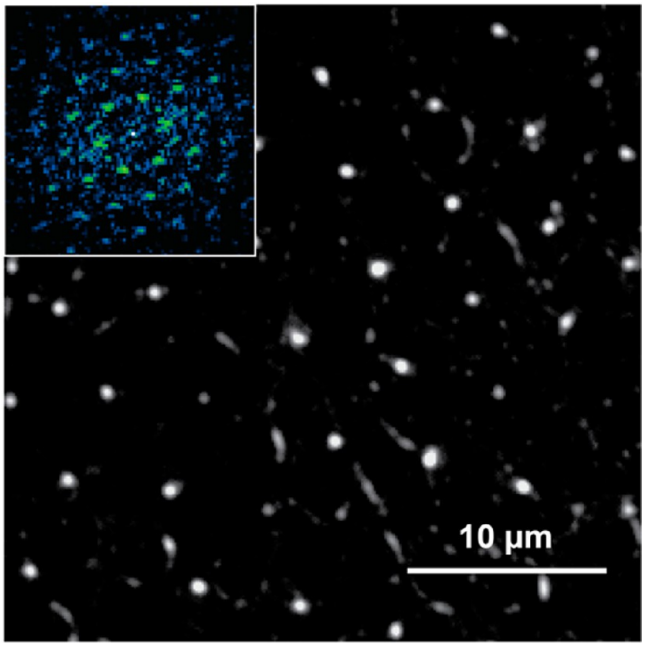

Figure 3. A fluorescence image of a 5 μm pattern functionalized with fluorescent BSA. Inset is the Fourier transform of the image.

sites was evident. There were also variations in intensity between attachment sites that may have been the result of variations in BSA attachment density or residue size. In negative control experiments without BSA or without the cross-linking reagents, no surface pattern was visible. However, we cannot rule out the possibility that noncovalent interactions between the protein and the polymer features contributed to the resulting surface patterns because some experiments failed to produce the expected pattern. We found that immersion in a hot water bath was the most effective and reproducible method for removing noncovalently adsorbed protein from the substrate, but in cases where heating is not possible, colloidal transfer printing could be combined with other surface blocking techniques.[4] We tested the deposition of a surface blocking oligo-ethylene glycol monolayer (OEG), but there was no improvement over the heated water removal and AFM images revealed multilayer deposition of the OEG.

CONCLUSION

We developed a new soft lithography technique, colloidal transfer printing, which can be used to produce an ordered array of polymer surface features with controlled size and spacing at submicrometer scales. A particular strength of this technique is that it does not require any specialized equipment. It only requires an oven and a sonicator, both of which are commonly found in wet-chemical laboratories. Colloidal transfer printing preserves many of the benefits of colloidal lithography, namely, the absence of a master, and complements other colloidal lithography methods by potentially requiring fewer processing steps. For example, to create a protein pattern like that in Figure 3 using established techniques would require several steps: deposition of a colloidal mask, deposition of a sacrificial layer through the mask, removal of the colloidal mask, backfilling with a reactive layer, and removal of the sacrificial layer. Due to its simplicity and minimal equipment requirements, we believe colloidal transfer printing could find wide use in biological and chemical fields that require a fast and inexpensive method to pattern large surface areas. The mechanism behind colloidal transfer printing is based on nonspecific particle−surface adhesion and particle cohesion, so the method should work with a wide variety of surfaces and particle chemistries. In the future, the use of standard surface functionalization techniques, like monolayer deposition,[34] and different colloidal particles[35] would greatly expand the number of possible surface patterns that could be produced with colloidal transfer printing.

ASSOCIATED CONTENT

Supporting Information

Supporting Figures S1−S7. This material is available free of charge via the Internet at http://pubs.acs.org.

AUTHOR INFORMATION

Corresponding Author

*E-mail: daniel.schwartz@colorado.edu.

Author Contributions

†M.J.S. and B.M.C. contributed equally.

Notes

The authors declare no competing financial interest.

ACKNOWLEDGMENTS

The authors acknowledge support from the U.S. Department of Energy Basic Energy Sciences, Chemical Sciences, Geosciences, and Biosciences Division (DE-SC0001854).

REFERENCES

(1) Lee, K.-B.; Park, S.-J.; Mirkin, C. A.; Smith, J. C.; Mrksich, M. *Science* **2002**, *295* (5560), 1702−1705.
(2) Whitesides, G. M. *Nat. Biotechnol.* **2003**, *21* (10), 1161−1165.
(3) Beaudet, A. L.; Belmont, J. W. *Annu. Rev. Med.* **2008**, *59*, 113−129.
(4) Falconnet, D.; Csucs, G.; Michelle Grandin, H.; Textor, M. *Biomaterials* **2006**, *27* (16), 3044−3063.
(5) Wong, J. Y.; Leach, J. B.; Brown, X. Q. *Surf. Sci.* **2004**, *570* (1), 119−133.
(6) Banerjee, P.; Bhunia, A. K. *Trends Biotechnol.* **2009**, *27* (3), 179−188.
(7) Ziegler, C. *Fresenius J. Anal. Chem.* **2000**, *366* (6−7), 552−559.
(8) Bhadriraju, K.; Chen, C. S. *Drug Discovery Today* **2002**, *7* (11), 612−620.
(9) Saavedra, H. M.; Mullen, T. J.; Zhang, P.; Dewey, D. C.; Claridge, S. A.; Weiss, P. S. *Rep. Prog. Phys.* **2010**, *73* (3), 036501.
(10) Gölzhäuser, A.; Eck, W.; Geyer, W.; Stadler, V.; Weimann, T.; Hinze, P.; Grunze, M. *Adv. Mater.* **2001**, *13* (11), 803−806.
(11) Chason, E.; Picraux, S. T.; Poate, J. M.; Borland, J. O.; Current, M. I.; Diaz de la Rubia, T.; Eaglesham, D. J.; Holland, O. W.; Law, M. E.; Magee, C. W.; Mayer, J. W.; Melngailis, J.; Tasch, A. F. *J. Appl. Phys.* **1997**, *81* (10), 6513−6561.
(12) Qin, D.; Xia, Y.; Whitesides, G. M. *Nat. Protoc.* **2010**, *5* (3), 491−502.
(13) Carlson, A.; Bowen, A. M.; Huang, Y.; Nuzzo, R. G.; Rogers, J. A. *Adv. Mater.* **2012**, *24* (39), 5284−5318.
(14) Li, F.; Josephson, D. P.; Stein, A. *Angew. Chem., Int. Ed.* **2011**, *50* (2), 360−388.
(15) Zhang, J.; Li, Y.; Zhang, X.; Yang, B. *Adv. Mater.* **2010**, *22*, 4249−4269.
(16) Li, J. R.; Lusker, K. L.; Yu, J. J.; Garno, J. C. *ACS Nano* **2009**, *3* (7), 2023−2035.
(17) Bognár, J.; Szűcs, J.; Dorkó, Z.; Horváth, V.; Gyurcsányi, R. E. *Adv. Funct. Mater.* **2013**, *23* (37), 4703−4709.
(18) Zhao, Z.; Cai, Y.; Liao, W.-S.; Cremer, P. S. *Langmuir* **2013**, *29* (22), 6737−6745.

(19) Garno, J. C.; Amro, N. A.; Wadu-Mesthrige, K.; Liu, G.-Y. *Langmuir* **2002**, *18* (21), 8186−8192.
(20) Yang, S. M.; Jang, S. G.; Choi, D. G.; Kim, S.; Yu, H. K. *Small* **2006**, *2* (4), 458−475.
(21) Haynes, C. L.; Van Duyne, R. P. *J. Phys. Chem. B* **2001**, *105* (24), 5599−5611.
(22) Hermanson, G. T. *Bioconjugate Techniques*, 2 ed.; Elsevier Inc.: Oxford, UK, 2008.
(23) Brandrup, J.; Immergut, E.; Grulke, E. *Polymer Handbook*, 4 ed.; Wiley: New York, 1999.
(24) Childs, W. R.; Nuzzo, R. G. *J. Am. Chem. Soc.* **2002**, *124* (45), 13583−13596.
(25) Barton, A. F. M. *CRC handbook of solubility parameters and other cohesion parameters*; CRC Press: Boca Raton, FL, 1983.
(26) Israelachvili, J. *Intermolecular and Surface Forces*, 3 ed.; Elsevier Inc.: Oxford, UK, 2011.
(27) Kono, R. *J. Phys. Soc. Jpn.* **1960**, *15* (4), 718−725.
(28) Taylor, Z. R.; Keay, J. C.; Sanchez, E. S.; Johnson, M. B.; Schmidtke, D. W. *Langmuir* **2012**, *28* (25), 9656−9663.
(29) Nam, H. J.; Jung, D.-Y.; Yi, G.-R.; Choi, H. *Langmuir* **2006**, *22* (17), 7358−7363.
(30) Gigault, C.; Dalnoki-Veress, K.; Dutcher, J. R. *J. Colloid Interface Sci.* **2001**, *243* (1), 143−155.
(31) Yoon, T.-Y.; Jeong, C.; Lee, S.-W.; Kim, J. H.; Choi, M. C.; Kim, S.-J.; Kim, M. W.; Lee, S.-D. *Nat. Mater.* **2006**, *5* (4), 281−285.
(32) Ogunyankin, M. O.; Huber, D. L.; Sasaki, D. Y.; Longo, M. L. *Langmuir* **2013**, *29* (20), 6109−6115.
(33) Nie, Z.; Kumacheva, E. *Nat. Mater.* **2008**, *7* (4), 277−290.
(34) Ulman, A. *Chem. Rev.* **1996**, *96* (4), 1533−1554.
(35) Xia, Y.; Gates, B.; Yin, Y.; Lu, Y. *Adv. Mater.* **2000**, *12* (10), 693−713.